2 The Essentials of Density Functional Theory and the Full-Potential Local-Orbital Approach

H. Eschrig

IFW Dresden, P.O.Box 27 00 16, 01171 Dresden, Germany

Abstract. Density functional theory for the ground state energy in its modern understanding which is free of representability problems or other logical uncertainties is reported. Emphasis is on the logical structure, while the problem of modeling the unknown universal density functional is only very briefly mentioned. Then, a very accurate and numerical effective solver for the self-consistent Kohn-Sham equations is presented and its power is illustrated. Comparison is made to results obtained with the WIEN code.

2.1 Density Functional Theory in a Nutshell

Density functional theory deals with inhomogeneous systems of identical particles. Its general aim is to eliminate the monstrous many-particle wave function from the formulation of the theory and instead to express chosen quantities of the system directly in terms of the particle density or the particle current density. There are basically three tasks: (i) to prove that chosen quantities are unique functionals of the density and to indicate how in principle they can be obtained, (ii) to find constructive expressions of model density functionals which are practically tractable and approximate the unique functionals in a way to provide predictive power, and (iii) to develop tools for an effective solution of the resulting problems.

As regards task (i), final answers have been given for the ground state energy [2.2, and citations therein]. In the following these results are summarized. Task (iii) is dealt with in the next section as well as in Chap. 3.

Central quantities of the *density functional theory for the ground state energy* are:

– the external potential $v(\boldsymbol{r})$ or its spin-dependent version

$$\check{v} = v_{ss'}(\boldsymbol{r}) = v(\boldsymbol{r})\delta_{ss'} - \mu_{\mathrm{B}}\boldsymbol{B}(\boldsymbol{r})\cdot\boldsymbol{\sigma}_{ss'}, \tag{2.1}$$

– the ground state density $n(\boldsymbol{r})$ or spin-matrix density

$$\check{n} = n_{ss'}(\boldsymbol{r}) \hat{=} \left\{ \begin{array}{l} n(\boldsymbol{r}) = \sum_s n_{ss}(\boldsymbol{r}), \\ \boldsymbol{m}(\boldsymbol{r}) = \mu_{\mathrm{B}} \sum_{ss'} n_{ss'}(\boldsymbol{r})\boldsymbol{\sigma}_{s's} \end{array} \right\}, \tag{2.2}$$

– the ground state energy

$$E[\check{v}, N] = \min_{\Gamma} \{ H_{\check{v}}[\Gamma] \mid N[\Gamma] = N \}. \tag{2.3}$$

H. Eschrig, The Essentials of Density Functional Theory and the Full-Potential Local-Orbital Approach, Lect. Notes Phys. **642**, 7–21 (2004)
http://www.springerlink.com/

Here, Γ means a general (possibly mixed) quantum state,

$$\Gamma = \sum_{M\alpha} |\Psi_{M\alpha}\rangle p_{M\alpha} \langle \Psi_{M\alpha}| \;, \quad p_{M\alpha} \geq 0 \;, \quad \sum_{M\alpha} p_{M\alpha} = 1 \tag{2.4}$$

where $\Psi_{M\alpha}$ is the many-body wave function of M particles in the quantum state α. In (2.3), $H_{\check{v}}[\Gamma]$ and $N[\Gamma]$ are the expectation values of the Hamiltonian with external potential $\check{v}$ and of the particle number operator, resp., in the state Γ. In the (admitted) case of non-integer N, non-pure (mixed) quantum states are unavoidable.

The variational principle by Hohenberg and Kohn states that there exists a density functional $H[\check{n}]$ so that

$$E[\check{v}, N] = \min_{\check{n}} \left\{ H[\check{n}] + (\check{v} \,|\, \check{n}) \;\middle|\; (\check{1} \,|\, \check{n}) = N \right\} \;, \tag{2.5}$$

$$(\check{v} \,|\, \check{n}) = \sum_{ss'} \int d^3r v_{ss'} n_{s's} = \int d^3r (vn - \boldsymbol{B} \cdot \boldsymbol{m}), \quad (\check{1} \,|\, \check{n}) = \sum_{s} \int d^3r n_{ss} \;. \tag{2.6}$$

Given an external potential $\check{v}$ and a (possibly non-integer) particle number N, the variational solution yields $E[\check{v}, N]$ and the minimizing spin-matrix density $\check{n}(\boldsymbol{r})$, the ground state density.

There is a unique solution for energy since $H[\check{n}]$ is convex by construction. The solution for $\check{n}$ is in general non-unique since $H[\check{n}]$ need not be strictly convex. The ground state (minimum of $H[\check{n}] + (\check{v} \,|\, \check{n})$) may be degenerate with respect to $\check{n}$ for some $\check{v}$ and N (cf. Fig. 2.1).

In what follows, only the much more relevant spin dependent case is considered and the checks above v and n are dropped.

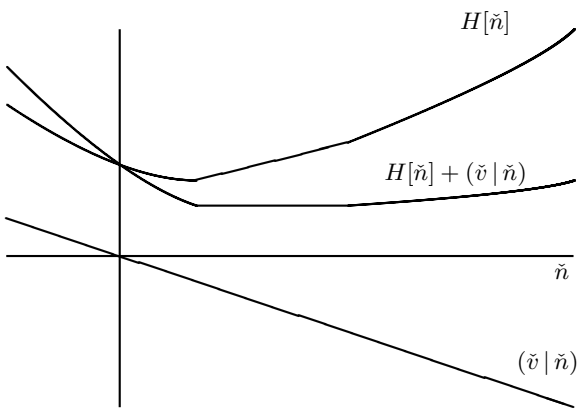

Fig. 2.1. The functionals $H[\check{n}]$, $(\check{v} \,|\, \check{n})$ and $H[\check{n}] + (\check{v} \,|\, \check{n})$ for a certain direction in the functional $\check{n}$-space and a certain potential $\check{v}$.

The mathematical basis of the variational principle is (for a finite total volume, for instance provided by periodic boundary conditions, to avoid formal difficulties with a continuous energy spectrum) that $E[v,N]$ *is convex in* N *for fixed* v *and concave in* v *for fixed* N*, and*

$$E[v+\text{const.},N] = E[v,N] + \text{const.}\cdot N. \tag{2.7}$$

Because of these simple properties of the ground state energy (which are not even mentioned by Hohenberg and Kohn in their seminal paper [2.5]) it can be represented as a double Legendre transform,

$$E[v,N] = \inf_n \sup_\mu \Big\{ H[n] + (v|n) + \big[N - (1|n)\big]\mu \Big\}, \tag{2.8}$$

which is equivalent to (2.5) because the μ-supremum is $+\infty$ unless $(1|n) = N$. The inverse double Legendre transformation yields the universal density functional:

$$H[n] = \inf_N \sup_v \big\{ E[v,N] - (n|v) \big\}. \tag{2.9}$$

Universality means that given a particle-particle interaction (Coulomb interaction between electrons say) a single functional $H[n]$ yields the ground state energies and densities for all (admissible) external potentials.

The expression (2.9) need not be the only density functional which provides (2.5). Generally two functions which have the same convex hull have the same Legendre transform. (Here the situation is more involved because of the intertwined double transformation.) Nevertheless, the outlined analysis can be put to full mathematical rigor, and the domain of admissible potentials is very broad and contains for instance the Coulomb potentials of arbitrary arrangements of nuclei. There are no representability problems. For details see [2.2].

This solves task (i) for the ground state energy as chosen quantity, which, for given v and N, is uniquely obtained via (2.5) from the functional $H[n] + (v|n)$. There are attempts to consider other quantities as excitation spectra or time-dependent quantities which are so far on a much lower level of rigor. Of course, $H[n]$ is unknown and of the same complexity as $E[v,N]$. It can only be modeled by guesses. This turns out to be uncomparably more effective than a direct modeling of $E[v,N]$.

Modeling of $H[n]$ starts with the Kohn-Sham (KS) parameterization [2.7] of the density by KS orbitals $\phi_k(\boldsymbol{r}s)$ and orbital occupation numbers n_k:

$$n(\boldsymbol{r}) = n_{ss'}(\boldsymbol{r}) = \sum_k \phi_k(\boldsymbol{r}s)\; n_k\; \phi_k^*(\boldsymbol{r}s'), \tag{2.10}$$

$$0 \le n_k \le 1, \quad \langle \phi_k | \phi_{k'} \rangle = \delta_{kk'}, \quad (1\,|\,n) = \sum_k n_k = N\,. \tag{2.11}$$

Model functionals consist of an orbital variation part K and a local density expression L:

$$\begin{aligned} H[n] &= K[n] + L[n] \ , \\ K[n] &= \min_{\{\phi_k, n_k\}} \Big\{ k[\phi_k, n_k] \Big| \textstyle\sum_k \phi_k n_k \phi_k^* = n \Big\} \ , \\ L[n] &= \int d^3 r n(\boldsymbol{r}) l\big(n_{ss'}(\boldsymbol{r}), \boldsymbol{\nabla} n, \dots\big) \ , \end{aligned} \tag{2.12}$$

which cast the variational principle (2.5) into the KS form

$$\begin{aligned} E[v, N] = \min_{\{\phi_k, n_k\}} \Big\{ & k[\phi_k, n_k] + L[\Sigma \phi n \phi^*] + (\Sigma \phi n \phi^* \,|\, v) \Big| \\ & \Big| \langle \phi_k | \phi_{k'} \rangle = \delta_{kk'}, 0 \le n_k \le 1, \textstyle\sum_k n_k = N \Big\} \ . \end{aligned} \tag{2.13}$$

ϕ_i^*, ϕ_i and n_i must be varied independently. The uniqueness of solution now depends on the convexity of $k[\phi_k, n_k]$ and $L[n]$.

Variation of ϕ_k^* yields the (generalized) KS equations:

$$\frac{1}{n_k} \frac{\delta k}{\delta \phi_k^*} + \Big(\frac{\delta L}{\delta n} + v \Big) \phi_k = \phi_k \epsilon_k \ . \tag{2.14}$$

Since n_k and ϕ_k^* enter in the combination $n_k \phi_k^*$ only, the relation

$$n_k \frac{\partial}{\partial n_k} = \Big\langle \phi_k \Big| \frac{\delta}{\delta \phi_k^*} \tag{2.15}$$

is valid which yields Janak's theorem:

$$\frac{\partial}{\partial n_k} \Big(k + L + (v \,|\, n) \Big) = \epsilon_k \ . \tag{2.16}$$

Variation of n_k, in view of the side conditions, yields the Aufbau principle: Let $n_{k'} < n_k$, then (cf. Fig. 2.2)

$$\delta n \Big(\frac{\partial}{\partial n_{k'}} - \frac{\partial}{\partial n_k} \Big) \Big(k + L + (v \,|\, n) \Big) \begin{cases} \ge 0 \text{ for } n_{k'} = 0 \text{ or } n_k = 1 \ , \\ = 0 \text{ for } 0 < n_{k'}, n_k < 1 \ . \end{cases} \tag{2.17}$$

Hence,

$$\begin{array}{ll} n_k = 1 & \text{for } \ \epsilon_k < \epsilon_N \ , \\ 0 \le n_k \le 1 & \text{for } \ \epsilon_k = \epsilon_N \ , \\ n_k = 0 & \text{for } \ \epsilon_k > \epsilon_N \ . \end{array} \tag{2.18}$$

Finding suitable expressions for k and L mainly by physical intuition is the way task (ii) is treated. The standard L(S)DA or GGA is obtained by putting

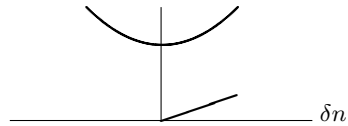

Fig. 2.2. A free minimum of a function of δn and a minimum under the constraint $\delta n > 0$.

$$k[\phi_k, n_k] = \sum_k n_k \langle \phi_k | - \frac{\nabla^2}{2} | \phi_k \rangle \; + \\ + \sum_{kk'} \frac{n_k n_{k'}}{2} \sum_{ss'} \int d^3r d^3r' \frac{|\phi_k(\boldsymbol{r}s)|^2 |\phi_{k'}(\boldsymbol{r}'s')|^2}{|\boldsymbol{r} - \boldsymbol{r}'|} \; . \tag{2.19}$$

This completes the brief introduction to the state of the art of density functional theory of the ground state energy.

Just to mention one other realm of possible density functionals, quasiparticle excitations are obtained from the coherent part (pole term) of the single particle Green's function ([2.3–2.5])

$$G_{ss'}(\boldsymbol{r}, \boldsymbol{r}'; \omega) = \sum_k \frac{\chi_s(\boldsymbol{r}) \eta^*_{s'}(\boldsymbol{r}')}{\omega - \varepsilon_k} + G^{\text{incoh}}_{ss'}(\boldsymbol{r}, \boldsymbol{r}'; \omega) \; , \tag{2.20}$$

$$\sum_{s'} \int d^3r' \Big[\delta(\boldsymbol{r} - \boldsymbol{r}') \Big(-\frac{\boldsymbol{\nabla}^2}{2} + u(\boldsymbol{r}) + u_{\text{H}}(\boldsymbol{r}) \Big) \\ + \Sigma_{ss'}(\boldsymbol{r}, \boldsymbol{r}'; \epsilon_k) \Big] \chi_{s'}(\boldsymbol{r}') = \chi_s(\boldsymbol{r}) \varepsilon_k \; . \tag{2.21}$$

Here, in the inhomogeneous situation of a solid, the self-energy Σ is among other dependencies a functional of the density. This forms the shaky ground (with rather solid boulders placed here and there on it, see for instance also [2.4]) for interpreting a KS band structure as a quasi-particle spectrum. In principle from the full $\Sigma_{ss'}(\boldsymbol{r}, \boldsymbol{r}'; \omega)$ the total energy might also be obtained.

2.2 Full-Potential Local-Orbital Band Structure Scheme (FPLO)

This chapter deals with task (iii) mentioned in the introduction to Chap. 1. A highly accurate and very effective tool to solve the KS equations self-consistently is sketched. The basic ideas are described in [2.6, see http://www.ifw-dresden.de/agtheo/FPLO/ for actual details of the implementation].

The KS (2.14) represents a highly non-linear set of functional-differential equations of the form

$$\hat{H}\phi_i = \Big[-\frac{\nabla^2}{2} + v_{\rm eff}\Big]\phi_i = \phi_i\epsilon_i \tag{2.22}$$

since the effective potential parts contained in $\delta k/\delta\phi_i^*$ and in $\delta L/\delta n$ depend on the solutions ϕ_i. The general iterative solving procedure is as follows:

Guess a density $n^{(\rm in)}_{ss'}(\boldsymbol{r})$.

- Determine the potentials $v_{\rm H}(\boldsymbol{r})$ (part of $\delta k/\delta\phi_i^*$ from the second line of (2.19)) and $v_{{\rm xc},ss'}(\boldsymbol{r}) = \delta L/\delta n_{s's}$.
- Solve the KS equation for $\phi_i(\boldsymbol{r}s), \epsilon_i$.
- Determine the density $n^{(\rm out)}_{ss'}(\boldsymbol{r}) = \sum_i \phi_i(\boldsymbol{r}s)\theta(\mu-\epsilon_i)\phi_i^*(\boldsymbol{r}s')$ with $\mu = \mu(N)$ from $\sum_i \theta(\mu-\epsilon_i) = N$.
- Determine a new input density $n^{(\rm in)}_{ss'}(\boldsymbol{r}) = f\big(n^{(\rm out)}_{ss'}(\boldsymbol{r}), n^{({\rm in},j)}_{ss'}(\boldsymbol{r})\big)$ from $n^{(\rm out)}$ of the previous step and $n^{({\rm in},j)}$ of a number of previous cycles; f has to be chosen by demands of convergence.

Iterate until $n^{(\rm out)} = n^{(\rm in)} = n^{(\rm SCF)}$.
SCF density: $n_{ss'}(\boldsymbol{r}) \hat{=} (n(\boldsymbol{r}), \boldsymbol{m}(\boldsymbol{r}))$,
Total energy: $E[v,N] = H[n] + (v\,|\,n)$.

In the following the most demanding second step is sketched.

2.2.1 The Local Orbital Representation

The KS orbitals $\phi_{\boldsymbol{k}n}$ of a crystalline solid, indexed by a wave number $\boldsymbol{k}$ and a band index n, are expanded into a nonorthogonal local orbital minimum basis (one basis orbital per band or per core state):

$$\phi_{\boldsymbol{k}n}(\boldsymbol{r}) = \sum_{\boldsymbol{R}\boldsymbol{s}L} \varphi_{\boldsymbol{s}L}(\boldsymbol{r}-\boldsymbol{R}-\boldsymbol{s}) C_{L\boldsymbol{s},\boldsymbol{k}n} e^{i\boldsymbol{k}(\boldsymbol{R}+\boldsymbol{s})}. \tag{2.23}$$

This leads to a secular equation of the form

$$HC = SC\epsilon\,, \tag{2.24}$$

$$H_{\boldsymbol{s}'L',\boldsymbol{s}L} = \sum_{\boldsymbol{R}} \langle \boldsymbol{0}\boldsymbol{s}'L'|\hat{H}|\boldsymbol{R}\boldsymbol{s}L\rangle e^{i\boldsymbol{k}(\boldsymbol{R}+\boldsymbol{s}-\boldsymbol{s}')}\,, \tag{2.25}$$

$$S_{\boldsymbol{s}'L',\boldsymbol{s}L} = \sum_{\boldsymbol{R}} \langle \boldsymbol{0}\boldsymbol{s}'L'|\boldsymbol{R}\boldsymbol{s}L\rangle e^{i\boldsymbol{k}(\boldsymbol{R}+\boldsymbol{s}-\boldsymbol{s}')}\,. \tag{2.26}$$

By definition, core states are local eigenstates of the effective crystal potential which have no overlap to neighboring core states and are mutually

orthogonal. This gives the overlap matrix (2.26) a block structure (indices c and v denote core and valence blocks) allowing for a simplified Cholesky decomposition into left and right triangular factors:

$$S = \begin{pmatrix} 1 & S_{cv} \\ S_{vc} & S_{vv} \end{pmatrix} = \begin{pmatrix} 1 & 0 \\ S_{vc} & S^L_{vv} \end{pmatrix} \begin{pmatrix} 1 & S_{cv} \\ 0 & S^R_{vv} \end{pmatrix} = S^L S^R \,, \tag{2.27}$$

$$S^L_{vv} S^R_{vv} = S_{vv} - S_{vc} S_{cv} \,. \tag{2.28}$$

The corresponding block structure of the Hamiltonian matrix (2.25) is

$$H = \begin{pmatrix} \epsilon_c 1 & \epsilon_c S_{cv} \\ S_{vc}\epsilon_c & H_{vv} \end{pmatrix}, \quad \epsilon_c = \mathrm{diag}(\cdots, \epsilon_{\boldsymbol{s}L_c}, \cdots) \,. \tag{2.29}$$

With these peculiarities the secular problem for H may be converted into a much smaller secular problem of a projected Hamiltonian matrix $\tilde{H}_{vv}$ as follows:

$$HC = SC\epsilon$$

$$(S^{L-1} H S^{R-1})(S^R C) = (S^R C)\epsilon$$

$$\Downarrow$$

$$\tilde{H}_{vv} \tilde{C}_{vv} = \tilde{C}_{vv} \epsilon_v \tag{2.30}$$

$$\tilde{H}_{vv} = S^{L-1}_{vv} (H_{vv} - S_{vc} H_{cc} S_{cv}) S^{R-1}_{vv}$$

$$C = \begin{pmatrix} 1 & -S_{cv} S^{R-1}_{vv} \tilde{C}_{vv} \\ & \\ 0 & S^{R-1}_{vv} \tilde{C}_{vv} \end{pmatrix} \,.$$

This exact reduction of the secular problem saves a lot of computer time in solving (2.25), by a factor of about 3 in the case of fcc Cu (with $3s, 3p$-states treated as valence states for accuracy reasons) up to a factor of about 40 in the case of fcc Au (again with $5s, 5p$-states treated as valence states). With slightly relaxed accuracy demands and treating the $3s, 3p$- and $5s, 5p$-states, resp., as core states, the gain is even by factors of 8 and 110.

2.2.2 Partitioning of Unity

The use of a local basis makes it desirable to have the density and the effective potential as lattice sums of local contributions. This is not automatically provided: the density comes out form summation over the occupied KS orbitals (2.22) as a double lattice sum, and the effective potential has anyhow a complicated connection with the KS orbitals. The decisive tool here is a partitioning of unity in $\boldsymbol{r}$-space.

There may be chosen:

- a locally finite cover of the real space $\mathbb{R}^3$ by compact cells Ω_i, that is, $\mathbb{R}^3 = \cup_i \Omega_i$ and each point of $\mathbb{R}^3$ lies only in finitely many Ω_i,
- a set of n-fold continuously differentiable functions $f_i(\boldsymbol{r})$ with $\mathrm{supp} f_i \subset \Omega_i$, that is $f_i(\boldsymbol{r}) = 0$ for $\boldsymbol{r} \notin \Omega_i$,
- $0 \leq f_i(\boldsymbol{r}) \leq 1$ and $\sum_i f_i(\boldsymbol{r}) = 1$ for all $\boldsymbol{r}$.

In the actual context, $\Omega_i = \Omega_{\boldsymbol{Rs}}$ indexed by atom positions.

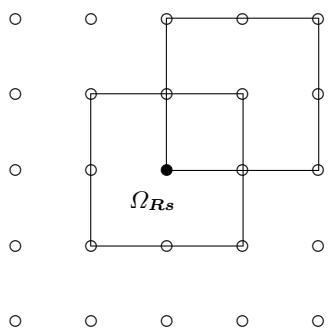

Fig. 2.3. A locally finite cover of the $\mathbb{R}^2$ by squares.

Figure 2.3 shows a locally finite cover of the plane by a lattice of overlapping squares.

2.2.3 Density and Potential Representation

The decomposition of the density

$$n(\boldsymbol{r}) = \sum_{\boldsymbol{Rs}} n_{\boldsymbol{s}}(\boldsymbol{r} - \boldsymbol{R} - \boldsymbol{s}) \tag{2.31}$$

is obtained by an even simpler one-dimensional partitioning along the line joining the two centers of a two-center contribution.

The potential is decomposed according to

$$v(\boldsymbol{r}) = \sum_{\boldsymbol{Rs}} v_{\boldsymbol{s}}(\boldsymbol{r} - \boldsymbol{R} - \boldsymbol{s}), \quad v_{\boldsymbol{s}}(\boldsymbol{r} - \boldsymbol{R} - \boldsymbol{s}) = v(\boldsymbol{r}) f_{\boldsymbol{Rs}}(\boldsymbol{r}) \tag{2.32}$$

with use of the functions f of the previous subsection.

Now, in the local items, radial dependencies are obtained numerically on an inhomogeneous grid (logarithmic equidistant), and angular dependencies are expanded into spherical harmonics (typically up to $l = 12$). To compute the overlap and Hamiltonian matrices, one has

– one-center terms: 1D numerical integrals,
– two-center terms: 2D numerical integrals,
– three-center terms: 3D numerical integrals.

2.2.4 Basis Optimization

The essential feature which allows for the use of a minimum basis is that the basis is not fixed in the course of iterations, instead it is adjusted to the actual effective crystal potential in each iteration step and it is even optimized in the course of iterations.

Take $\bar{v}_{\boldsymbol{s}}$ to be the total crystal potential, spherically averaged around the site center $\boldsymbol{s}$. Core orbitals are obtained from

$$(\hat{t} + \bar{v}_{\boldsymbol{s}})\varphi_{\boldsymbol{s}L_c} = \varphi_{\boldsymbol{s}L_c}\epsilon_{\boldsymbol{s}L_c} \ . \tag{2.33}$$

Valence basis orbitals, however, are obtained from a modified equation

$$\left(\hat{t} + \bar{v}_{\boldsymbol{s}} + \left(\frac{r}{r_{\boldsymbol{s}L_v}}\right)^4\right)\varphi_{\boldsymbol{s}L_v} = \varphi_{\boldsymbol{s}L_v}\epsilon_{\boldsymbol{s}L_v} \ . \tag{2.34}$$

The parameters $r_{\boldsymbol{s}L_v}$ are determined by minimizing the total energy. There are two main effects of the $r_{\boldsymbol{s}L_v}$-potential:

– The counterproductive long tails of basis orbitals are suppressed.
– The orbital resonance energies $\epsilon_{\boldsymbol{s}L_v}$ are pushed up to close to the centers of gravity of the orbital projected density of states of the Kohn-Sham band structure, providing the optimal curvature of the orbitals and avoiding insufficient completeness of the local basis.

In the package FPLO the optimization is done automatically by applying a kind of force theorem during the iterations for self-consistency.

2.2.5 Examples

In order to illustrate the accuracy of the approach, the simple case of fcc Al is considered. Figure 2.4 shows the dependence of the calculated total energy

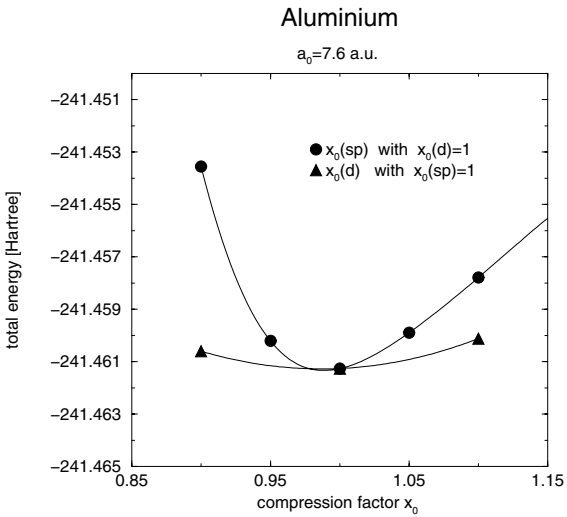

Fig. 2.4. Total energy of aluminum as a function of the parameters $x_0 = r_0/r_{\mathrm{NN}}^{3/2}$.

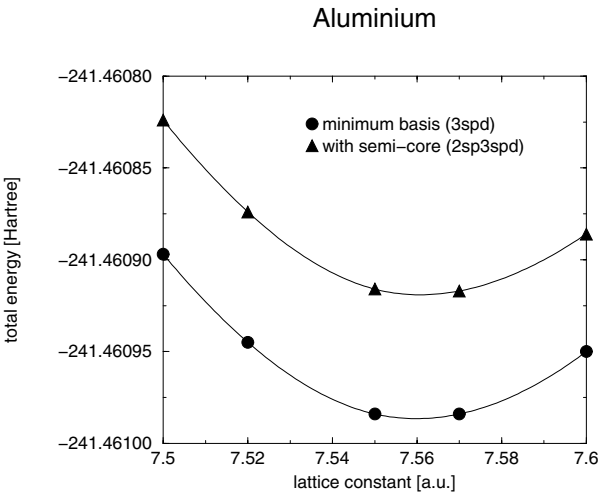

Fig. 2.5. Total energy vs. lattice constant of aluminum for two basis sets.

as a function of the basis optimization parameters $x_0(L_v) = r_{L_v}/r_{NN}^{3/2}$ while Fig. 2.5 shows the effect of treating the $2s, 2p$-states either as core states or as valence states (called semi-core states in the latter case). Note that neglecting the neighboring overlap of $2s, 2p$-states is an admitted numerical error and not a question of basis completeness; the more accurate total energy in this case is the higher one with the semi-core treatment.

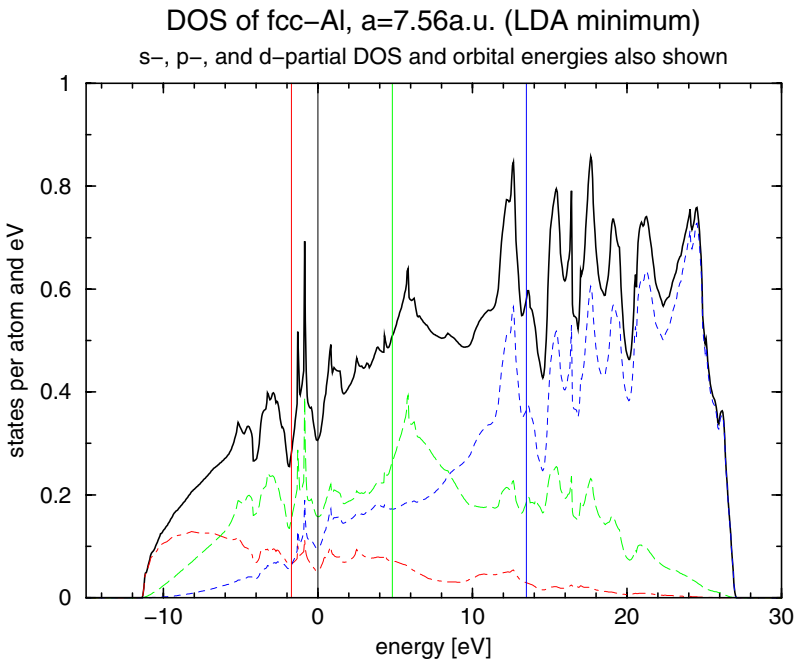

Fig. 2.6. DOS and l-projected DOS of aluminum; the vertical lines indicate the orbital resonance energies.

Next, in Fig. 2.6 the density of states (DOS) and the orbital projected DOS of Al are shown. (The energy zero here and in the following is put at the Fermi level.) Vertical lines mark the basis orbital resonance energies ϵ_{L_v} of (2.34). As a result of optimizing the parameters r_{L_v} of this equation, clearly the energies are close to the centers of gravity of the corresponding projected DOS. This proves optimization of basis completeness within the fixed number of basis orbitals. Even the down shift of ϵ_d from the corresponding center of gravity of the d density of states is correct since completeness is needed only in the lower, occupied part.

For illustration, the KS band structure of Al is shown on Fig. 2.7. Remarkably, the third band is above the Fermi level at point W: The LDA Fermi surface of Al has the right topology and is quantitatively very correct (Fig. 2.8). The frequently asserted failure of the LDA not to produce the right FS topology of Al is a muffin-tin problem.

On Fig. 2.9 it is illustrated on the example of Sr_2CuO_3 how the automate basis optimization works; x_0 steps are those self-consistency steps which adjust the x_0 parameters. The corresponding convergence of the total energy is also shown.

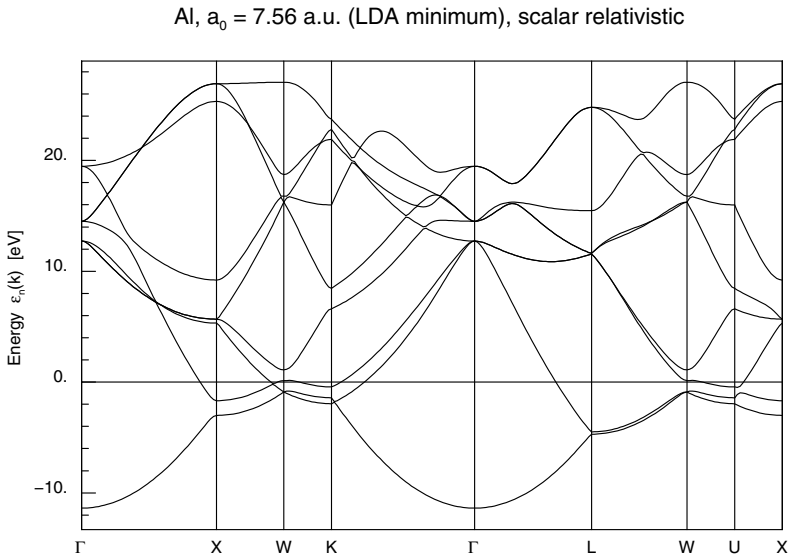

Fig. 2.7. KS band structure of aluminum.

Fig. 2.8. LDA Fermi surface of aluminum.

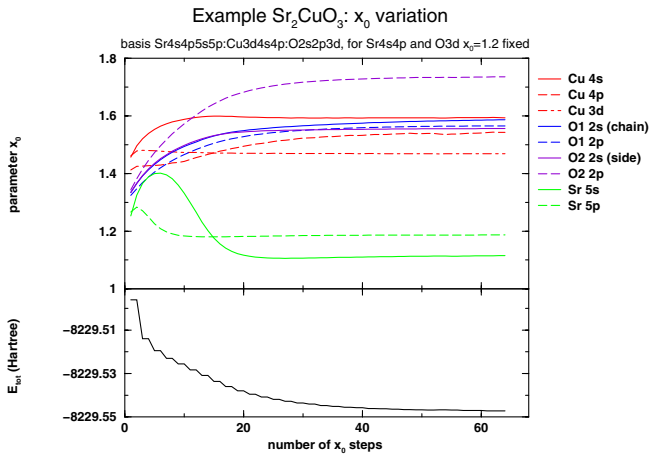

Fig. 2.9. Automatic basis optimization for Sr_2CuO_3 in the course of iterations.

For this example, the position of the basis orbital resonance energies relative to the corresponding orbital projected DOS are shown on Fig. 2.10. The same correlation as for Al is observed.

2.2.6 Comparison of Results from FPLO and WIEN97

To get some feeling on the absolute accuracy of calculated total energies, a number of comparisons is made between results obtained with exactly the same density functional (occasionally very slightly different from the previous examples) but with solvers working with totally different basis sets: augmented plane waves vs. local orbitals. The results were carefully converged within both approaches: in WIEN97 [2.1] with the number of plane waves (far beyond the default) and in FPLO with basis optimization and generally including $3d$ polarization orbitals for oxygen.

On Fig. 2.11 the obtained densities of states for $CaCuO_2$ are presented. The FPLO basis was

Ca: $\{1s, 2s, 2p\}_c$, $\{3s, 3p, 3d, 4s, 4p\}_v$
Cu: $\{1s, 2s, 2p\}_c$, $\{3s, 3p, 3d, 4s, 4p\}_v$
O: $\{1s\}_c$, $\{2s, 2p, 3d\}_v$.

The differences are mainly due to a different $\boldsymbol{k}$-integration routine used in the codes to calculate the density of states from the band energies.

Table 1 contains the absolute values of total energies obtained with both approaches for a number of elemental metals and compounds. The agreement is to our knowledge unprecedented so far which speaks of the quality of both codes.

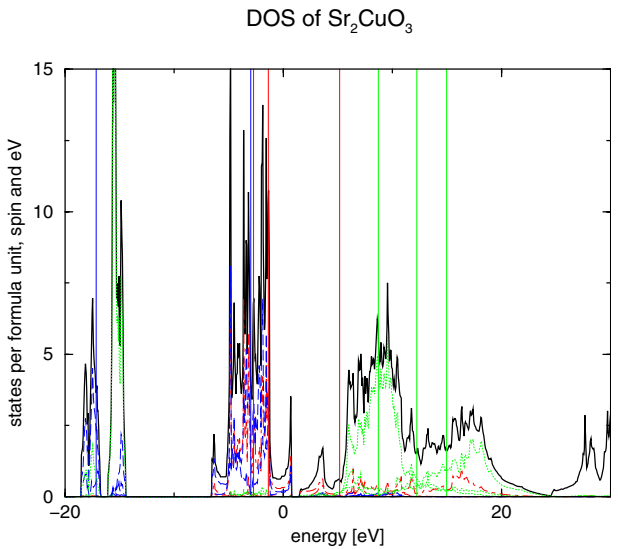

Fig. 2.10. DOS and l-projected DOS of Sr_2CuO_3; vertical lines indicate orbital resonance energies. dashed line: O $2s, 2p$; dot-dashed line: Cu $3d, 4s, 4p$; dotted line: Sr $4d, 5s, 5p$ in ascending order of energies.

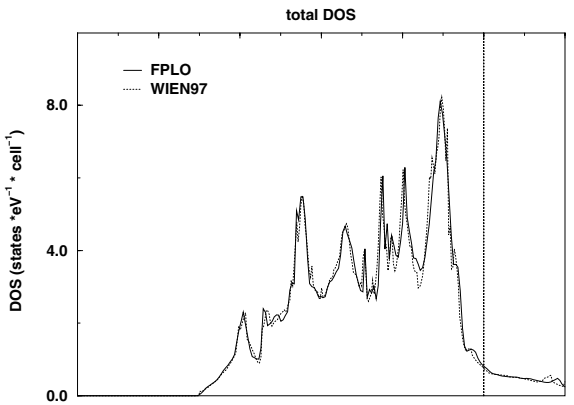

Fig. 2.11. Comparison of the DOS of $CaCuO_2$ from FPLO and from WIEN97.

It should be mentioned that due to the extremely small basis of FPLO the computing time for matrix algebra and diagonalization does not dominate the total computing time even for rather large unit cells: up to at least 100 atoms per cell the time scales roughly as $N^{1.5}$ which allows for instance for large numbers of $\boldsymbol{k}$ points where this is needed.

A fully relativistic four-component version and a flexible CPA implementation for substitutional alloys are available.

Table 2.1. Total energies: (Al, Fe, Ni non-relativistic, all others scalar-relativistic)

solid	N	E_{FPLO} [Hartree]	E_{WIEN} [Hartree]	$\Delta E/N$ [mHartree]
fcc-Al	1	-241.464 0	-241.465 5	1.5
FM-bcc-Fe	1	-1 261.456 5	-1 261.457 2	0.7
FM-fcc-Ni	1	-1 505.875 5	-1 505.877 -	1.5
fcc-Cu	1	-1 652.483 2	-1 652.484 1	0.9
$CaCuO_2$	4	-2 480.992 6	-2 480.995 5	0.7
Sr_2CuO_3	6	-8 229.534 4	-8 229.544 1	1.6
$Sr_2CuO_2Cl_2$	7	-9 075.266 6	-9 075.286 3	1.4
Cu_2GeO_4	14	-11 400.481 1	-11 400.503 6	1.6

Acknowledgements

In preparing this text, many discussions with M. Richter, K. Koepernik, H. Rosner and U. Nitzsche were of great help.

References

[2.1] P. Blaha, K. Schwarz, and J. Luitz. WIEN'97, a full potential linearized augmented plane wave package for calculating crystal properties. Technical report, Technical University of Vienna, 1999.

[2.2] H. Eschrig. *The Fundamentals of Density Functional Theory.* Edition am Gutenbergplatz, Leipzig, 2003.

[2.3] L. Hedin. New method for calculating the one-particle green's function with application to the electron-gas problem. *Phys. Rev.*, 139:A796–A823, 1965.

[2.4] L. Hedin and B.I. Lundqvist. Explicit local exchange and correlation potentials. *J. Phys. C: Solid St. Phys.*, 4:2064–2083, 1971.

[2.5] P. Hohenberg and W. Kohn. Inhomogeneous electron gas. *Phys. Rev.*, 136:B864–B871, 1964.

[2.6] K. Koepernik and H. Eschrig. Full-potential nonorthogonal local-orbital minimum-basis band-structure scheme. *Phys. Rev.*, B59:1743–1757, 1999.

[2.7] W. Kohn and L.J. Sham. Self-consistent equations including exchange and correlation effects. *Phys. Rev.*, 140:A1133–A1138, 1965.